Journal of Chemical Technology and Metallurgy, 58, 6, 2023, 1100-1106

NON-EQUILIBRIUM PROCESSES IN THE ATMOSPHERE, WATER, AND REACTIONS WITH CALCIUM CARBONATE IN THE ENVIRONMENT

Ignat Ignatov[1], Mario Iliev[2], Plamen Gramatikov[3,4], Alexander Ignatov[1],
Mariana Angelcheva[5], Ivan Angushev[6], Christos Drossinakis[7]

[1]Scientific Research Center of Medical Biophysics
N. Kopernik str., 32, Sofia 1111, Bulgaria
[2]Faculty of Physics, Sofia University "St. Kliment Ohridski"
Sofia 1000, Bulgaria
[3]Department of Green Energetics
European Polytechnical University
23 Sv. Sv. Kiril i Metodiy Str., Pernik 2300;
[4]Physics Department, South-West University "Neofit Rilski"
Blagoevgrad 2700, Bulgaria
[5]Department of Kinesitherapy and Rehabilitation
National Sports Academy, "V. Levski", Sofia 1700, Bulgaria
[6]Medical University-Sofia 1606, Bulgaria
[7]IAWG-INTERNATIONALE Akademie für Wissenschaftliche Geistheilung
Frankfurt, Germany; Hauptplatz 44, 2293 Marchegg 2293, Austria
E-mail: mbioph@abv.bg

Received 23 March 2023
Accepted 20 May 2023

ABSTRACT

Non-equilibrium processes in the atmosphere and water were described in this paper. Spectral analysis by NES and DNES methods was applied to research water structure. The energy spectrum of water is obtained due to the non-equilibrium process of evaporation of water drops. The term Non-equilibrium energy spectrum (NES) is used in this method. The distribution function according to hydrogen bond energies f(E) is measured in reciprocal electron volts (eV^{-1}). The differential energy spectrum DNES represents the difference between the investigated sample's NES and the control sample's NES. It is assumed that the combined influence of all factors other than those under study is identical for the control and sample. The effects of gas-solid heat exchange and calcium carbonate ($CaCO_3$) decomposition were described. Our research aims to show peaks at 713 and in the 873 - 879 cm^{-1} due to shared environmental influences on calcium carbonate. The purpose of the article is to demonstrate that by studying the spectral parameters at 713 and in the range of 873 ÷ 879 cm^{-1}, an assessment can be made for the application of the impact of water with different physicochemical parameters, air humidity, thermal effects on the quality of lime mortar solutions and chemical processes with carbon dioxide (CO_2).

Keywords: calcium carbonate, water, NES, DNES, FTIR.

INTRODUCTION

In the nature, calcium carbonate ($CaCO_3$) interacts in land-water-air contact environments. Due to the changes in environmental conditions such as temperature, humidity, and geophysical fields, the authors choose the DNES spectral method, with which they study a sample and a control sample. Differential Non-equilibrium Energy Spectrum (DNES) measures the alteration of the structure of water due to the influence because it is assumed that the combined influence of the remaining factors besides the examined one is identical for the control sample and the sample. NES and DNES methods range from λ from 8 to 14 μm and $\tilde{v}$ from 1250 to 714 cm^{-1}. In the same range, the highest level of polarization of infrared radiation is observed in absorption and reflection from water (~ 4 - 10 %) [1]. The research was performed with Fourier Transform Infrared (FT-IR) method λ from 2.5 to 25 μm and $\tilde{v}$ from 4000 to 400 cm^{-1}.

For estimation of non-equilibrium conditions with $CaCO_3$, were analyzed the effects of cave water [2], gas-solid heat exchange [3], developing CO_2 capture, and using technologies to reduce anthropogenic emissions as part of the solutions against climate change [4], global dioxide emissions [4].

Our studies aim to analyze the impact of a total Solar eclipse on the water spectrum and the similarity of the peaks with solutions of $CaCO_3$ on the peaks. The analysis also was performed for 39 studies of water samples for the duration of one year. The results with water from Rupite Basin, Bulgaria, rich in Ca^{2+}, HCO_3^-, and CO_3^{2-}.

EXPERIMENTAL

Materials and methods

Spectral methods Non-equilibrium energy spectrum (NES) and Differential non-equilibrium energy spectrum (DNES)

The wetting angle θ was measured with a specially designed instrument described in detail in [5 - 7]. Evaporation of deionized water drops was performed in a sealed chamber with a stable temperature of 22°C [5, 8] (Fig. 1). The drops were placed on a 350 µm thick BoPET (biaxially-oriented polyethylene terephthalate) sheet.

The device has the following technical features:

- Monochromatic filter with wavelength $\lambda = 580 \pm 7$ nm;
- Water evaporation angle ranging from 72.3 deg to 0 deg.
- Measured range of energy of hydrogen bonds among water molecules is $\lambda = 8.9 - 13.8$ µm or $E = (-0.08) - (-0.1387)$ eV.

Luck considers that in water, there are hydrogen bonds between the hydrogen atom of one water molecule and the oxygen of another [9]. Most of them are bound by the energy of the connection (-E), and the remaining are free (E = 0). It is accepted that E has a negative value. This is Luck's two-state model [10 - 13]. Each water molecule has two hydroxide groups. The number of hydrogen bonds between the hydrogen atom of one water molecule and the oxygen of another in a particular volume of water is twice as high as the number of molecules it contains.

Part of the hydrogen bonds is restructured in the proximity of the spherical part of the drop surface and, as a result, we obtain the dependence between the surface tension δ and the hydrogen bond energy [8, 14-16]:

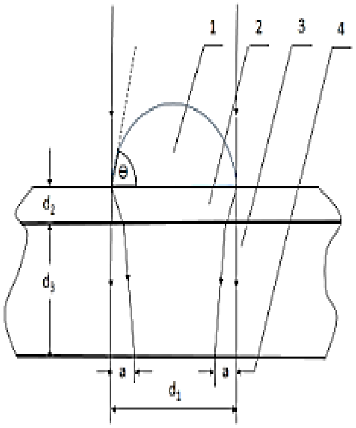

Fig. 1. Operating principle of the method for measuring the wetting angle of liquid drops on a hard surface: 1- drop, 2 - thin Maylar sheet, 3 - glass plate, 4 - refraction ring width. The wetting angle θ is a function of **a** and $\mathbf{d_1}$.

The equation can describe the relationship:

$$\delta = -kTI\ln[1+\alpha/[\exp(-\beta E)+\alpha]] \quad (1)$$

Here, k is the Boltzmann constant, $\beta = 1/kT$, T – is the absolute temperature, E – the hydrogen bond energy, α is the ratio of two subvolumes of the phase space related to the structuring and restructuring of hydrogen bonds, $\alpha = 28 \pm 8$, and $I = 5.03.10^{18}$ m^{-2} is the density of water molecules in the hydrophobic surface layer.

The values of E and α are determined by comparison with the experiment. Expression (1) explains the fraction C of the actual surface tension γ, i.e., $\delta = C\gamma$ [15]. According to [8, 15], the contribution of the non-hydrogen bond interaction amounts to 20 % of the actual value of γ and C = 4/5.

The Helmholtz free surface energy (F) can be defined as $F = \gamma\Sigma$, where Σ represents the spherical part of the droplet surface [8]. At the mechanical equilibrium point, F should be minimized, which can be expressed as $dF = 0 = d(\gamma\Sigma)$ [8]. Consequently, we have the equation:

$$0 = \gamma\Sigma - \gamma_0\Sigma_0 \quad (2)$$

The forced evaporation process of water drops occurs at a constant temperature of 20°C within a sealed chamber [5].

The expressions for Σ_0 and Σ are given by [8]:

$$\Sigma = \pi D^2/2(1 + \cos\theta);\ \Sigma_0 = \pi D^2/2(1 + \cos\theta_0) \quad (3)$$

$$-E/kT = C\gamma/IkT \quad (4)$$

$$E = C\gamma_o(1 + \cos\theta) / (I (1 + \cos\theta_0)) \tag{5}$$

During the evaporation process, the wetting angle (θ) undergoes discrete changes and represents the average energy of hydrogen bonds as follows:

$$\theta = \arccos(-1 + bE), \text{ where } b = I (1 + \cos\theta_0)/(C\gamma o) \tag{6}$$

where θ is the wetting angle, E is the average energy of hydrogen bonds, and b is a temperature-dependent parameter [17 - 20]. The development of the method is the Non-equilibrium energy spectrum (NES) and Differential non-equilibrium spectrum (DNES) [20 - 24]. They are used to research natural waters and plants [25 - 29]. Molecular dynamics simulation is applied to investigate the wetting behavior of water droplets on the sandstone surface under different salinities. The system equilibrium configuration was used to study the interaction of its components. The number of hydrogen bonds was calculated [30, 31].

The energy (E) of hydrogen bonds among H_2O molecules in water samples is measured in eV. The function f(E) is called the *energy distribution spectrum*. A non-equilibrium evaporation process of water droplets characterizes the energy spectrum of water. This non-equilibrium energy spectrum (NES) is measured in eV^{-1}. DNES is defined as the difference [18 - 20, 32]:

$$\Delta f (E) = f (\text{water sample}) - f (\text{control water sample}) \tag{7}$$

DNES is measured in eV^{-1} where *f (*)* denotes the evaluated energy [14 - 18].

IR-Spectroscopy

IR-spectra of calcium carbonate ($CaCO_3$) was registered with Fourier Transform Infrared (FTIR) method with the device Thermo Nicolet Avatar 360 Fourier-transform IR.with spectral range average IR – 400 - 4000 cm^{-1}; the permission - 0.5 cm^{-1};

RESULTS AND DISCUSSION

Results with Non-equilibrium energy spectrum (NES) and Differential non-equilibrium energy spectrum (DNES)

A study on August 11, 1999, of the total solar eclipse was done by methods of NES and DNES. The research was performed on August 10, a day before the solar eclipse. The meteorological parameters were temperature in degree centigrade (°C) and relative humidity in percents (%). During the solar eclipse on August 11, the meteorological parameters were – t_{max} = 29.7°C and RH_{max} = 57 %. On August 10, the meteorological parameters were t_{max} = 36.3°C and RH_{max} = 27 % [33]. The results of f (E) in eV^{-1} are shown in Table 1. The difference of f(E) was describe at (E = -0.1012 eV)(λ = 12.3 μm)(ṽ = 816 cm^{-1}) and (E = -0.1087 eV) (λ =

Table 1. The function of the distribution of energies f(E) in eV^{-1} for the function of distribution of energies f(E) according to the value of (-E) of hydrogen bonds during the total Solar eclipse (11.08.1999) as a sample and deionized water as a control sample.

-E(eV) x-axis	Deionized Water Total Solar eclipse f(E) (eV^{-1})	Deionized Water Control sample f(E) (eV^{-1})	-E(eV) x-axis	Deionized Water Total Solar eclipse f(E) (eV^{-1})	Deionized Water Control Sample f(E) (eV^{-1})
0.0937	0	30.1	0.1187	15.1	0
0.0962	23.1	0	0.1212	30.2	30.2
0.0987	23.1	38.5	0.1237	0	15.1
0.1012	0	46.2	0.1262	15.1	30.2
0.1037	30.2	38.5	0.1287	15.1	30.2
0.1062	0	30.2	0.1312	30.1	23.1
0.1087	15.1	46.2	0.1337	15.1	23.1
0.1112	46.2	0	0.1362	46.2	0
0.1137	15.1	23.1	0.1387	76.9	0
0.1162	0	23.1	–	–	–

11.41 μm) ($\tilde{v}$ = 877 cm^{-1}). Line positions, strengths, and absolute energies are calculated for the pure rotational spectrum of water evaporation in the region between 0 and 877 cm^{-1} [34]. During a solar eclipse, alterations in non-stationary heat fluxes to the Earth were proven [35].

Table 1 illustrates the function of the distribution of energies f(E) according to the values of (-E) of hydrogen bonds during the total Solar eclipse as a sample and deionized water as a control sample [36].

At λ from 8 to 14 μm and $\tilde{v}$ from 1250 cm^{-1} to 714 cm^{-1}, the highest level of polarization of infrared radiation is observed in absorption and reflection from water (~ 4 - 10 %) [1].

With the method, NES performed 39 independence measurements in one year. With an arrow designated, the average value of the energy between the water molecules was determined as value E = -1090 eV or (λ = 11.38 μm) ($\tilde{v}$ = 879 cm^{-1}) (Fig. 2) [2].

A horizontal arrow is designated the window of the transparency of the Earth's atmosphere for the electromagnetic radiation in the middle infrared range of the Sun towards the Earth and from our planet towards the surrounding cosmic space. The range is at λ from 8 to 14 μm and $\tilde{v}$ from 1250 cm^{-1} to 714 cm^{-1} [37].

There is designated one of the expressed peaks at $\tilde{v}$ = 795 cm^{-1} or (E = -0.099 eV) (λ = 12.58 μm) of the energy of hydrogen bonds [38].

E_M = -0.1389 eV (λ = 8.93 μm) ($\tilde{v}$ = 1120 cm^{-1}) is the hydrogen bond energy used in the model of Luzar et al. [11] and determined by spectroscopic measurement [39].

The results show that the value $\tilde{v}$ = 877 cm^{-1} - 879 cm^{-1} alterations were connected with alterations in environmental conditions.

Results of reactions with calcium carbonate ($CaCO_3$)

The effects of gas-solid heat exchange and calcium carbonate decomposition were proved at (λ = 11.41 μm) ($\tilde{v}$ = 877 cm^{-1}) [3].

In our research with the method Fourier-IR spectrometer [39, 40], the peaks were at $\tilde{v}$ = 713 cm^{-1} and $\tilde{v}$ = 873 cm^{-1} (Fig. 3) [40 - 41].

The research was performed with sediments from mineral water from Rupite, Bulgaria. In 2020 the number of hydrogencarbonate ions (HCO_3^-) was 1495 - 1526, and of calcium (Ca^{2+}) was 31.6 - 40.2 mg L^{-1} [42]. Fig. 4 illustrates peaks at $\tilde{v}$ = 713 cm^{-1} and $\tilde{v}$ = 875 cm^{-1}. The following reaction is valid:

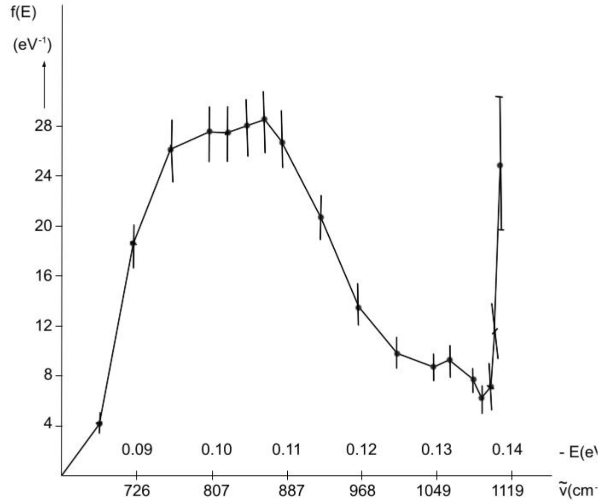

Fig. 2. Results with method NES have performed 39 independence measurements in a period of one year.

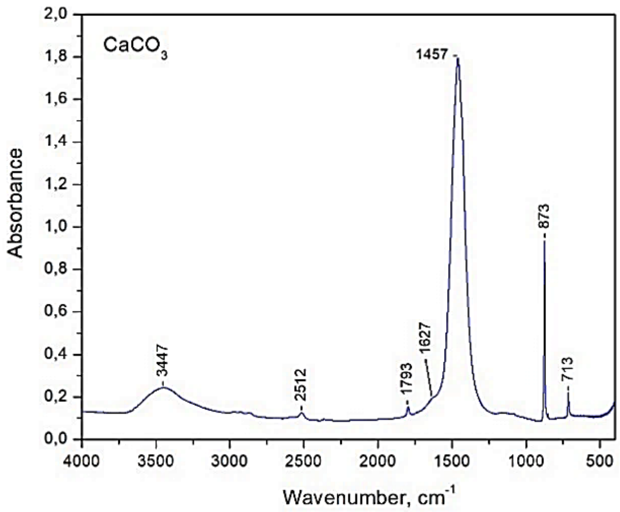

Fig. 3. Result of calcium carbonate ($CaCO_3$) with Fourier-IR spectrometer.

$$2HCO_3^- + Ca^{2+} \rightarrow CaCO_3 + CO_2 + H_2O \quad (8)$$

The lime cycle is

$$CaCO_3 \rightarrow CaO \rightarrow Ca(OH)_2 \rightarrow CaCO_3 \quad (9)$$

The chemical reaction (8) is a significant emitter of global dioxide emissions [43]. With the research of 713 and in the range 873 cm^{-1} - 879 cm^{-1} is possible to estimate the influence on the environment and select the optimal value for the industry. Developing CO_2 capture and using technologies to reduce anthropogenic emissions can be part of the solution against climate change [4].

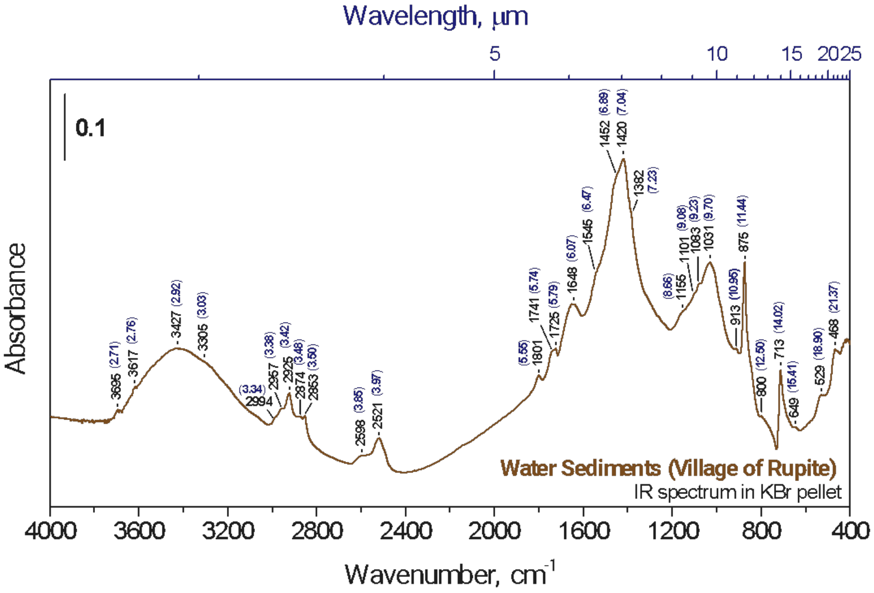

Fig. 4. Result with sediments from Rupite, Bulgaria, with Fourier-IR spectrometer.

CONCLUSIONS

Processes in the atmosphere, water, and such with calcium carbonate ($CaCO_3$) were examined, looking for regularity of spectral characteristics.

Non-equilibrium processes in the atmosphere and water were described in the publication. For water research, spectral analysis with NES and DNES methods was applied.

During the solar eclipse on 11.08.1999, a difference was observed between the deionized water control sample of 10.08.1999 and the sample of 11.08.1999 at (E = -0.1087 eV) (λ = 11.41 µm)(ṽ = 877 cm^{-1}).

An examination was conducted of 39 deionized water samples. The average value of the energy of the hydrogen bonds among water molecules is (E = -0.1090 eV) (λ = 11.38 µm) (ṽ = 879 cm^{-1}).

DNES was studied of water from the “Temnata dupka” (Dark Hole) cave with values of calcium ions (Ca^{2+}) 66 mg L^{-1} and hydrogencarbonate ions (HCO_3^-) content of 223 mg L^{-1}. An extremum was observed at (E = -0.1087 eV)(λ = 11.41 µm) (ṽ = 877 cm^{-1}). Fourier spectral analysis was performed of $CaCO_3$ with the following results (E = 0.1082 eV) (λ = 11.46 µm) (ṽ = 873 cm^{-1}). The spectral range of water vapor is also from 0 to 877 cm^{-1}. The adsorption peaks of the lime are at 713 cm^{-1} and 875 cm^{-1}. The results indicate that an analysis of peaks at 713 and within the interval of 873 ÷ 879 cm^{-1} can be used to evaluate non-equilibrium processes with calcium carbonate in water and in contact with air. As a result of exposure to water with different physicochemical parameters, air humidity, and thermal effects, the quality of lime mortar solutions and protection against carbon dioxide emissions can be assessed.

The optical low-power method of investigation by analysis of NES and DNES applied in this paper. It is confirmed that IR methods could be a suitable tool for fast analyses of changes in water structure and properties after outer influences.

Acknowledgements

The article is in the memory of Prof. Anton Antonov (1934-2021).

REFERENCES

1. J.A. Shaw, Degree of linear polarization in spectral radiances from water-viewing infrared radiometers. Applied Optics, 38, 15, 1999, 3157-3165.
2. A. Antonov, Research of the non-equilibrium processes

in allocated systems, Dissertation thesis for degree “Doctor of physical sciences”, Blagoevgrad, Sofia, 1995, 1-255.

3. M. Galvan, J. Hernandez. Characterization of Calcium Carbonate, Calcium Oxide, and Calcium Hydroxide as starting point to improving lime for their use in construction, Journal of Materials and Civil Engineering, 21, 11, 2009.
4. M. Ozekmekci, M. Copur, Synthesis of $CaCO_3$ and trimethyl borate by reaction of ulexite and methanol in the presence of CO_2. Journal of CO_2 utilization, 42, 2021, 101321.
5. A. Antonov, L. Yuskesselieva, Method for determination of structural changes in liquids, Author’s certificate of invention, 1983, 43821.
6. A. Antonov, An optical method version for determination of the welling angle of liquids. Comptes Rendus de l’Académie Bulgare des Sciences, 37, 1984, 1199.
7. A. Antonov, L. Yuskesselieva, I. Teodossieva, Influence of ions on the structure of water under conditions far away from equilibrium. Physiologie, 26, 1989, 2552.
8. L. Todorova, A. Antonov, Note on the drop evaporation method for studying water hydrogen bond distribution: I. An application for filtration, Comptes Rendus de l’Académie Bulgare des Sciences, 53, 2000, 43-46.
9. W. Luck, A model of hydrogen-bonded liquids, Angewandte Chemie, 19, 1980, 28-41.
10. G.M. Kontogeorgis, A. Hoster, N. Kottaki, E. Tsochantaris, F. Topsoe, J. Poulsen, M. Bache, X. Liang, N. S. Blom, J. Kronholm, Water structure, properties and some applications - a review, Chemical Thermodynamics and Thermal Analysis, 6, 2022, 100053.
11. L.F. Vega, F. Llovell, Review and new insights into applying molecular-based equations of state to water and aqueous solutions, Fluid Phase Equilibria, 416, 2016, 150-173.
12. S. Aparicio-Martínez, K. Hall, Phase equilibria in water containing binary systems from molecular-based equations of state. Fluid Phase Equilibria, 254, 2007, 112-125.
13. G. Clark, A. Haslam, A. Galindo, G. Jackson, Developing optimal Wertheim - models of water for use in statistical associating fluid theory (SAFT) and related approaches. Molecular Physics, 104, 2010, 3561-3581.
14. B. Zhang, J. Kim, T. Ch. Lee, Behavior of an evaporating water droplet on a lubricant-impregnated nano-structured surface, Experimental Thermal and Fluid Science, 96, 2018, 96, 216-223.
15. A. Luzar, S. Svetina, B. Žekš, The contribution of hydrogen bonds to the surface tension of water, Chemical Physics Letters, 96, 1983, 485-490.
16. P.S. Gramatikov, A.S. Antonov, On the two conditions model of water structure. Comptes Rendus de l’Académie Bulgare des Sciences, 50, 3, 1997, 13-16.
17. A. Kumbharkhane, Y.S. Joshi, S.C. Mehrotra, Sh. Yagihara, S. Sudo, Study of hydrogen bonding and thermodynamic behavior in water–1,4-dioxane mixture using time domain reflectometry, Physic B: Condensed Matter, 421, 2013, 1-7.
18. P.S. Gramatikov, A. Antonov, M. Gramatikova, Study of the properties and structure variations of water systems under the stimulus of outside influences, Fresenius Journal of Analytical Chemistry, 343, 1992, 134-135.
19. S. Todorov, A. Damianova, I. Sivriev, A. Antonov, T. Galabova, Water energy spectrum method and investigation of the variations of the H-bond structure of natural waters, Comptes Rendus de l ‘Academie Bulgare des Sciences, 61, 2008, 857-862.
20. S. Todorov, A. Damianova, A, Antonov, L. Todorova, Investigations of natural waters spectra from the Rila mountain national park lakes, Comptes Rendus de l ‘Academie Bulgare des Sciences, 63, 2010, 555-560.
21. I. Ignatov, G. Gluhchev, N. Neshev, D. Mehandjiev, Structuring of water clusters depending on the energy of hydrogen bonds in electrochemically activated waters Anolyte and Catholyte, Bulgarian Chemical Communications, 53, 2021, 234-239.
22. S. Boteva, A. Kenarova, G. Radeva, I. Traykov, V. Bogoev, Community dynamics of pelagic bacteria in the high mountain lake Bubreka, Rila mountain. Bulgaria, Comptes Rendus de l’Académie Bulgare des Sciences, 66, 2013, 1579-1586.
23. N. Neshev, I. Ignatov, R. Toshkova, Ch. Drossinakis, G. Gluhchev, Hydrogen bonds energy distribution and information-theoretic analysis of blood serum from hamsters with experimental Graffi tumor, Libri Oncologici, 50, 2-3, 2022, 52-61.
24. D. Mehandjiev, I. Ignatov, N. Neshev, P. Vassileva, G. Gluhchev, F. Huether, Ch. Drossinakis, History-dependent hydrogen bonds energy distributions

in NaCl aqueous solutions undergoing osmosis and diffusion through a ceramic barrier, J. Chem. Technol. Metall., 58, 2, 2023, 340-346.

25. I. Ignatov, T. P. Popova, Applications of Moringa oleifera Lam., Urtica dioica L., Malva sylvestris L., and Plantago major L. containing potassium for recovery, Plant Cell Biotechnol Mol Biol J., 22, 7-8, 2021, 93-103.
26. I. Ignatov, N. Valcheva, Physicochemical, isotopic, spectral, and microbiological analyses of water from glacier Mappa, Chilean Andes, Journal of the Chilean Chemical Society, 68, 1, 2023, 5802-5906.
27. I. Ignatov, V. Balabanski, M. Angelcheva, Application of infrared spectral analyses for medicinal plants containing Calcium (Ca^{2+}), Plant Science Today, 9, 2022, 1066 -1073.
28. I. Ignatov, N. Neshev, T. P. Popova, Y. Kiselova-Kaneva, Ch. Drossinakis, R. Bankova, R. Toshkova, G. Gluhchev, N. Valcheva, M. Angelcheva, G. Dinkov, I. Angushev, T. Todorova, V. Balabanski, S. Baiti, F. Huether, A.I. Ignatov, Theoretical analysis of hydrogen bonds, energy distribution and information in a 1 % Rosa damascena Mill oil solution, Plant Science Today, 9, 3, 2022, 760-765.
29. F. Huether, I. Ignatov, Y. Kiselova-Kaneva, T. P. Popova, R. Bankova, N. Neshev, G. Gluhchev, S. Karadzhov, N. Valcheva, P. Vassileva, A. I. Ignatov, I. Angushev, T. Todorova, M. Angelcheva, Results obtained with EVOagri technology to improve yield using filtered water in Africa, Tibet, Italy and Bulgaria, Plant Science Today, 10, 2, 2023.
30. T. Yu, Q. Li, H. Hu, Y. Tan, L. Xu, Molecular dynamics simulation of the interfacial wetting behavior of brine/sandstone with different salinities, Colloid and Surfaces A: Physicochemical and Engineering Aspects, 632, 2022, 127807.
31. G. Yitian, F. Hongwei, K. Ni, A Hierarchical clustering method of hydrogen bond networks in liquid water undergoing shear flow, Scientific Reports, 11, 2021, 9542.
32. D. Mehandjiev, I. Ignatov, N. Neshev, F. Huether, G. Gluhchev, Ch. Drossinakis, Formation of clusters in water and their distribution according to the number of water molecules, Bulgarian Chemical Communications, 54, 3, 2022, 211-216.
33. I. Ignatov, A. Antonov, T. Galabova, K. Avramov, The total solar eclipse on 11 August 1999 and research by biophysical model systems, Seminar “Man and Nature”, SRCMB, Sofia, Teteven, 2021, 42-44.
34. J.K. Messer, F.C. De Lucia, P. Helminger, The pure rotational spectrum of water vapor - A millimeter, submillimeter, and far infrared analysis, Int J Infrared Milli Waves, 4, 1983, 505-539.
35. O. N. Boitman, A. D. Kalikhman, A. V. Tashchilin, The midlatitude ionosphere during the total solar eclipse of March 9, 1997, 104, A12, 1999, 28197-28206.
36. I. Ignatov, F. Huether, N. Neshev, Y. Kiselova-Kaneva, T. P. Popova, R. Bankova, N. Valcheva, A. I. Ignatov, M. Angelcheva, I. Angushev, S. Baiti, Research of water molecules cluster structuring during Haberlea rhodopensis Friv. hydration, Plants, 2022, 11, 19, 2655.
37. T.J. Wallington, M.P.S. Andersen, O.J. Nielsen, Relative integrated IR absorption in the atmospheric window differs from relative radiative efficiency. Proceeding of National Academy of Sciences, 107, 48, 2010, E178-E179.
38. S.L. Chang, T.-M. Wu, Instantaneous normal mode analysis of orientation motions in liquid water: Local structural effects. Journal of Chemical Physics, 121, 2004, 3605.
39. N. Biliškov, Infrared spectroscopic monitoring of solid-state processes. Physical Chemistry Chemical Physics, 32, 2022.
40. D. Panayotov, V. Zdravkova, O. Lagunov, S. Andonova, I. Spassova, D. Nihtianova, G. Atanasova, N. Drenchev, E. Ivanova, M. Mihaylov, K. Hadjiivanov. Capturing CO_2 by ceria-zirconia nanomaterials of different origin. Physical Chemistry Chemical Physics. 2023.
41. I. Ignatov, T.P. Popova, T. Petrova, A.I. Ignatov, Physicochemical Parameters and in vitro Antimicrobial Effects of Water Filtrated with Nano-structured Carbonaceous Shungite, J. Chem. Technol. Metall., 57, 5, 2022, 937-947.
42. I. Ignatov, Origin of life and living matter in hot mineral water and properties of polar molecules in the primary hydrosphere and hydrothermal ponds, Uttar Pradesh Journal of Zoology, 42, 6, 2021, 37-52.
43. Zh. Bian, Y. Li, Y. Ren, Y. Fang, J. Zhao, Thermochemical heat storage performance of CaO particles under fluidization in coupled $CaO/Ca(OH)_2$ cycles and $CaO/CaCO_3$ cycles, Journal of Energy Storage, 56, B, 2022, 106045.